Materials Science in Semiconductor Processing 74 (2018) 1–6

Contents lists available at ScienceDirect

Materials Science in Semiconductor Processing

journal homepage: www.elsevier.com/locate/mssp

Interface and transport properties of gamma irradiated Au/n-GaP Schottky diode

N. Shiwakoti[a], A. Bobby[a], K. Asokan[b], Bobby Antony[a,*]

[a] Department of Applied Physics, Indian Institute of Technology (ISM) Dhanbad, 826004, India
[b] Inter University Accelerator Centre, Aruna Asaf Ali Marg, New Delhi 110067, India

ARTICLE INFO

Keywords:
Au/GaP Schottky diode
Gamma irradiation
Current transport
Interface
Capacitance

ABSTRACT

The effect of 10 Mrad γ-ray exposure on the interface and transport properties of Au/n-GaP Schottky diode is studied in the 220–400 K temperature range. There is significant alteration in the interface and defect state density after irradiation. The Arrhenius plot of σ_{ac} shows the presence of both shallow and deep trap states corresponding to activation energies 0.073 eV and 0.21 eV respectively. The influence of additional defects is reflected in the charge transport mechanism at low temperature regimes, where tunneling mechanisms are observed. The perceived transport and capacitance/conductance properties are ascribed due to further interfacial and deep defect state formation upon gamma irradiation.

1. Introduction

The radiation resistant electronic components are persistently probed by researchers due to their increasing concerns related to the stability of devices in radiation harsh environments. The continuous exposure of radiation to these devices especially in the field of space crafts, military aircrafts, artificial satellites, nuclear reactors, particle accelerators etc. usually ruin their functionality in due time. Besides, the thermal stability of these devices under radiation environment should also be meticulously considered for wide range applications. The choice of suitable materials under such backdrop is a prime need of growing technology. The Gallium Phosphide (GaP) based junction devices shows some potential features such as low leakage current, high break down voltage, robust thermal stability etc [1–4]. Its use as light emitting diodes, U-V radiation detectors [5,6] and more advanced structures such as window layer of heterojunction solar cells [7,8] etc. draws a level of attention on its reliability and efficiency under radiation harsh environments. The superiority of this wide band gap semiconductor is numerous over Si and other compound semiconductors. It can operate competently as a bipolar device in extended temperature range [1]. Recently, an increase in quantum efficiency of Ni/n-GaP Schottky diode by nano scale surface formation is reported [9]. The simplest of all junction devices is MS or Schottky device, which is investigated both as electronic device and for material characterization [6,10]. Fundamentally, all these devices are common in one aspect. Their terminal characteristics are governed by the interface conditions. Any kind of alterations of the MS interface state properties due to external influences reflect directly on their terminal behaviors. So a thorough understanding of interface states profile is crucial for their feasibility under harsh environments. The effect of γ-ray irradiation is one of such concern which requires systematic investigations in GaP based devices. Furthermore, the high penetrating power of γ-ray is also employed as an effective tool for altering the MS interface state properties [11–14]. The fate of the device after irradiation primarily depends on how the interface state density and defect state energy levels are modulated. The gamma ray irradiation can induce both transient and permanent effects within the device [14–16]. Upon bombardment, the gamma ray photons generate electron-hole pairs which may either recombine or move out of the interface. When an external field is applied, the electrons from the pairs are swept across the interface whereas the holes, being less mobile get trapped and form stationary trap states. In addition, the gamma ray photons may lose energy by photoelectric and Compton scattering processes depending on their energy values. These processes generate high energy electrons which subsequently interact with the atoms of the device, forming some stable point defects or annihilating the existing defects. Such interactions can also change the electronic configuration of the atoms leading to restructuring and reordering of the interface which releases lattice strain and homogenizes interfacial regions causing improvement in device performance [17]. They may also provide tunneling channel for the free charge carriers [18–21]. Thus, at different biases and temperatures, these defect states actively control the free carrier density and mobility and hence affect the transport mechanisms. In GaP crystal, there exist point defects such as phosphorous vacancy (V_P), gallium vacancy (V_G),

* Corresponding author.
E-mail address: bobby.iit.ism@gmail.com (B. Antony).

http://dx.doi.org/10.1016/j.mssp.2017.10.008
Received 30 May 2017; Received in revised form 11 September 2017; Accepted 8 October 2017

gallium-phosphors divacancy with different charge states, phosphorus gallium antisite (P_{Ga}), unintentional impurities and lattice dislocations [22–26]. Upon irradiation, these existing defects along with interface states due to contact inhomogeneity and surface impurities form defect complexes, which change the device characteristics drastically. Several groups have investigated the radiation response of different kinds; such as Swift heavy ion [27–29], electron irradiation [30–32], neutron irradiation [33], γ-ray irradiation [32] on the surface and bulk properties of GaP single crystals. Mostly, all kinds of radiation increase the interface states density which leads to device degradation [34,35]. However, the effect of such irradiation on device structures, particularly of GaP based ones, and their possibility in radiation environment is still in the premature stage.

This work is an extension of our previous works on pristine Au/n-GaP under the influence of gamma irradiation [36,37]. In this work, we have investigated the interface state modification and the related charge transport properties through *C-V* and *I-V* characterization techniques measured at room temperature (RT).

2. Experimental

The Au/n-GaP Schottky diode was fabricated and the detailed description of device structure and measurement techniques has been presented earlier [37]. The diode so fabricated was irradiated with 10 Mrad ^{60}Co γ - ray source installed at IUAC, New Delhi.

3. Results and discussion

3.1. Capacitance and conductance characteristics

The capacitance and conductance measurements are effective tools in understanding the interface state density and carrier life time along with activation energy of defect states. The interfacial states accompanied by series resistance arise due to various reasons. One of which is the unwanted growth of an ultrathin interfacial oxide layer at the metal-semiconductor junction during fabrication, particularly in III-V semiconductor based Schottky diode. The *C-V* and G/ω-*V* characteristics of gamma irradiated Au/n-GaP Schottky diode at different frequencies are shown in Figs. 1 and 2. The capacitance and conductance values decrease in comparison with the pristine diode indicating formation of extra defect levels after irradiation. It is quite normal in such Schottky diodes to observe anomalous peaks in their *C-V-f* characteristics [41,42], which is alike in our case too (Fig. 1). As majority of the interface states cannot follow high frequencies, the interface capacitance decreases with increasing frequency, thereby lowering the total capacitance. The *G/ω-V* plot in Fig. 2 shows drastic change in its characteristic over high to low frequency ramping. The effect of deep

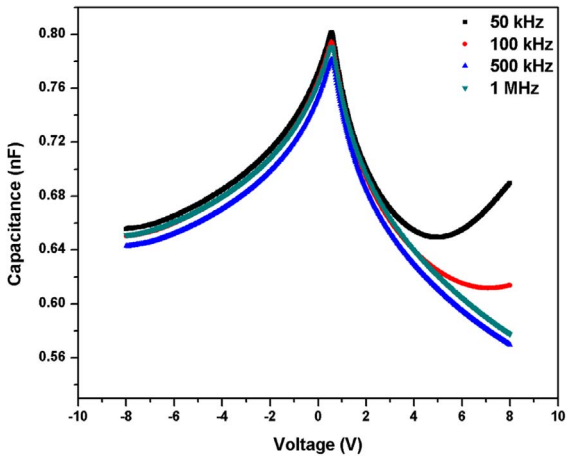

Fig. 1. C–V characteristics of γ-ray irradiated Au/n-GaP Schottky diode measured at RT.

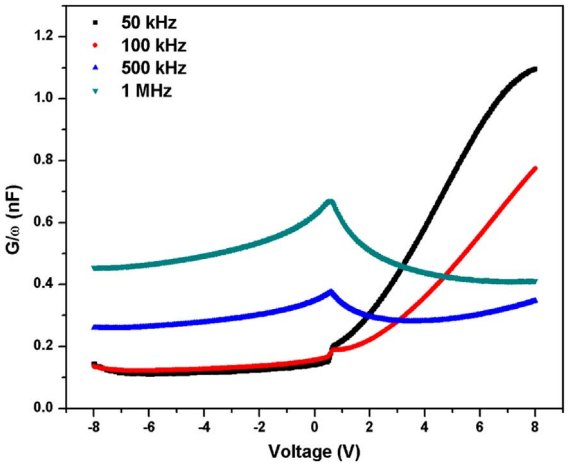

Fig. 2. G/ω-V characteristics of γ-ray irradiated Au/n-GaP Schottky measured at RT.

defect level is visible from the low frequency conductance characteristics at high forward bias region. Under sufficiently strong bias, the deep defect levels are activated, which then can communicate with neighboring interface states effectively at low frequencies and hence increases the conductance. However, the increase in conductance with increase in frequency in the reverse bias region can be looked upon due to particular distribution of the interface states and increase in series resistance after irradiation [44]. The conductance is the measure of various component of a.c. tunnel current, mainly due to potential fluctuation at the semiconductor surface, charging and discharging current at the interface states and the recombination current in the space charge region. Unlike for the pristine sample [37], the increase in conductance with increase in frequency indicates the formation of radiation induced recombination centers or defects which promote recombination current in the space charge region. Furthermore, the conductance may also increase if charging and discharging current or hopping conduction process increases at the interface due to increase in interface state density. The increase in proximity of the interface states may cause well synchronization of the interface states charging and discharging processes even under the influence of high frequency a.c field. In other words, there exists continuum distribution of interface sates with varying time constants.

3.2. Bias dependent interface state analysis

The measured capacitance and conductance values are used to evaluate parallel conductance (G_P) from Nicollian and Brews method [37,43]. The $G_p/\omega - f$ plot under different biases at RT (Fig. 3) exhibits a peak, whose magnitude and position depend on the gate bias voltage. The peak position shifts towards higher frequency region as the bias voltage is incremented from 0 V to 0.6 V, which however, starts shifting towards lower frequency region with further rise in bias voltage. This reverse peak shift is absent in the reported pristine sample [37]. Moreover, the peak value of G_p/ω decreases as the bias voltage increases except at 0.8 V. The bias dependent shift of $G_p/\omega - f$ peaks suggest a change in the time constant of interfaces states. This can be attributed to the particular distribution of the interface state energy levels responding independently with varying bias.

The same G_p/ω – frequency plot is used to evaluate the interface state density (N_{ss}) and relaxation time (τ) as described previously in detail [37]. The values of N_{ss} and the τ are plotted against E_c-E_{ss} as shown in Fig. 4. The E_c and E_{ss} represent energy levels corresponding to the bottom of the conduction band and energy of the interface states respectively.

The value of N_{ss} increases gradually towards the mid of the bandgap varying from $0.58 \times 10^{13}\,eV^{-1}\,cm^{-2}$ to $1.27 \times 10^{13}\,eV^{-1}\,cm^{-2}$,

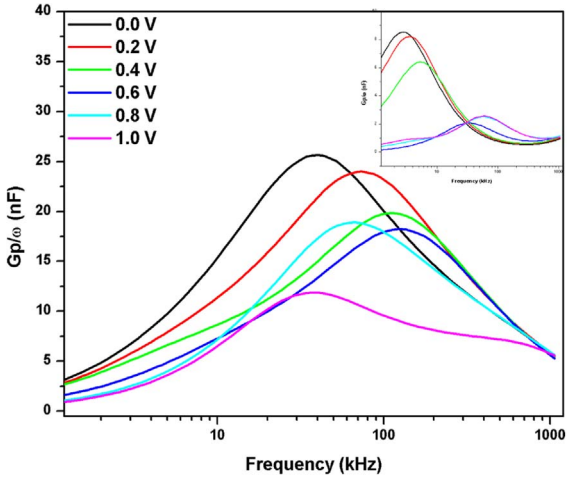

Fig. 3. (i) Frequency dependence G_p/ω for γ-ray irradiated Au/n-GaP Schottky diode evaluated at different biases (ii) Inset shows frequency dependence G_p/ω for pristine sample.

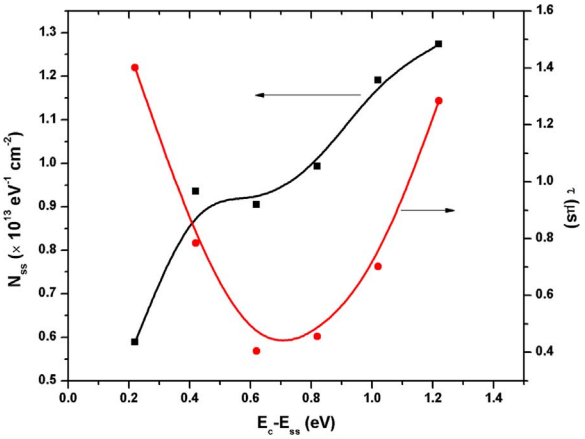

Fig. 4. Distribution plots of interface states density (N_{ss}) and their time constant (τ) for γ-ray irradiated Au/n-GaP Schottky diode at RT; At ≈ 0.7 eV, the N_{ss} shows a subtle change with minima in τ value.

where the variation is subtle in the range 0.4–0.8 eV. In this region, the interface states are expected to communicate with the deep trap levels under forward bias, elucidating the observed conductance behavior. As stated earlier, one of the major components of charge conduction for the observed frequency dependence of conductance is due to electric field driven and thermally assisted charge carrier hopping. The uniformly distributed and closely spaced interface states in this region can promote short range hopping mechanism of charge carriers which contributes to high frequency conductance. On the other hand, the conductance at low frequency can be looked upon due to long range hopping of charge carries among the interface states and the deep defects. In addition, the recombination current due to added defect centers may also prevail in parallel with the hopping mechanism to consistently explain the frequency dependence conductance behavior. The value of τ is high for the interface states lying close to the bottom of the conduction band and it falls rapidly attaining a minima at around 0.7 eV; which again starts increasing as the energy level approaches the mid of the bandgap. However, the dip in τ value was not present in the pristine sample [37]. The time constant generally decreases when the interface states are in close proximity with Fermi level. Furthermore, the charge carriers are mediated faster through the defects while it encounters with the later, if any, during the bias sweep. Hence, the exhibition of minima in τ infers the presence of deep defect levels in the irradiated sample that are different from the pristine. The values of τ in

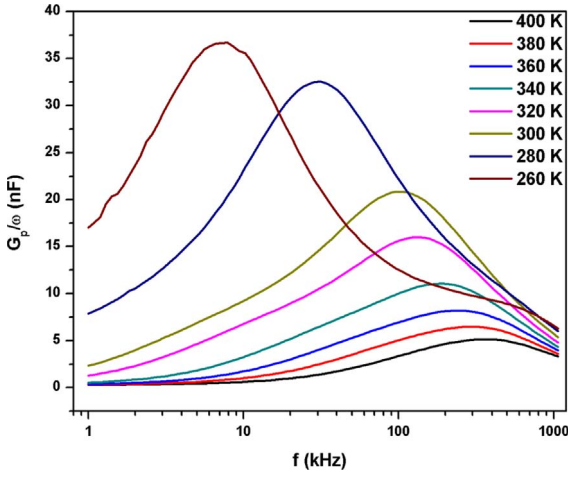

Fig. 5. Frequency dependence G_p/ω for γ-ray irradiated Au/n-GaP Schottky diode evaluated at different temperature.

the irradiated sample vary from 0.43μs to 1.4μs, whereas in pristine sample the variation is from 0.85μs to 18.19μs. The reduction in the span of τ after gamma irradiation indicates the annihilation of some of the defects having high relaxation time.

3.3. Temperature dependent interface state analysis

The temperature dependent G_p/ω-f plot ranging from 260 to 400 K range measured at 0.2 V bias is shown in Fig. 5. It exhibits a broad peak at each temperature that signifies the existence of non Debye type relaxation process with wide distribution having individual time constant. This accounts for the frequency invariance of C-V characteristics under forward and moderate reverse bias. The peak position shifts towards lower frequency as the temperature decreases, suggesting lattice rearrangement with longer relaxation time of the interface states.

The N_{ss} and τ associated with varying temperature depicted in Fig. 6 also shows prominent variation. The obtained value of N_{ss} at 300 K is 1.03×10^{13} eV^{-1} which is higher by an order of magnitude as reported for the pristine sample [37]. In the present case N_{ss} decreases gradually with increase of temperature, which indicates annihilation of some of the defects, either existing or gamma induced, at high temperatures. As the temperature increases, the mobility of charge carriers increases due to their faster movement among the trap states. This causes reduction in relaxation time.

The evaluation of the temperature dependent ac electrical conductivity (σ_{ac}) from the conductance measurements was used to

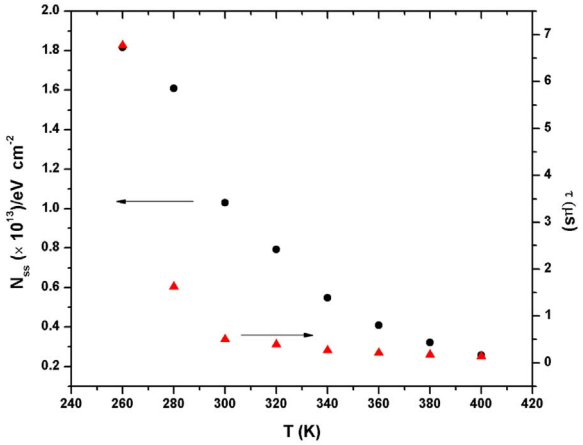

Fig. 6. Temperature dependence of N_{ss} and τ for γ-ray irradiated Au/n-GaP Schottky diode.

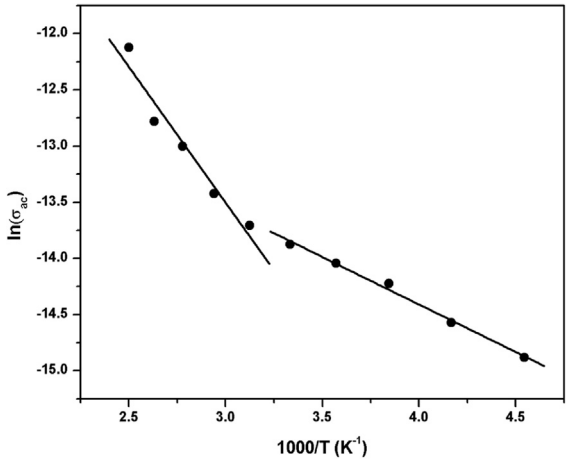

Fig. 7. Arrhenius plot of γ-ray irradiated Au/n-GaP Schottky diode in the temperature range of 220–400 K. The graph reveals the existence of shallow defect level of 0.073 eV and deep defect level of 0.21 eV.

calculate the activation energy of the trap states [37]. Its relation with temperature is expressed as $\sigma_{ac} = \sigma_o \exp(-E_a/kT)$; where E_a is the activation energy of the trap states. The plot of $ln(\sigma_{ac})$ with the inverse of T, also known as the Arrhenius plot, should be a straight line whose slope can be used to determine E_a.

In the present case, however the Arrhenius plot in Fig. 7 shows two linear regions corresponding to the activation energies 0.073 eV and 0.21 eV respectively. These activation energies suggest the presence of both shallow and deep trap states. From our previous study of pristine sample, three distinct energy levels of shallow trap states corresponding to activation energies of 0.013, 0.034, and 0.061 eV were reported [37]. The extracted values of E_a indicate that the shallow trap states which lie just below the conduction band are largely altered. In addition, deep trap states are also formed in the device after gamma irradiation. Although a deep defect level of 0.21 eV has been detected from the plot, the characteristic variation of τ in Fig. 4 indicates the presence of other defect levels of higher energies. These additional defect states largely influences the current transport processes, which has been covered in the following section.

3.4. Analysis of current transport mechanisms

The forward and reverse I-V characteristics of the gamma irradiated Au/n-GaP under different temperatures is shown in Fig. 8. It is clear that the diode exhibits good rectifying characteristics even after gamma irradiation. The rectification ratio (RR) measured at ± 0.58 V is 32.48 which shows degradation in the irradiated diode as compared to the pristine diode. This is true at other measured temperatures also. The forward bias current of the diode is the exponential function of the applied voltage in the intermediate voltage range which shows two distinct behaviors depending on the bias range. At higher bias voltage (above 0.7 V) the *I-V* characteristics deviates significantly due to the series resistance. Similar type of I-V nature is also reported in other Schottky structure [45–47]. Preliminary analyses of the temperature dependent forward I-V data were done assuming the usual thermionic emission process based on an intimate Au/n-GaP contact. However, the curves could not be fitted consistently under this assumption which indicated presence of other conduction processes beside thermionic emission. The curves could be well fitted using the modified thermionic emission (TE) and tunneling (TN) equations by considering presence of an ultra-thin native oxide layer on the GaP surface. It suggests that the native oxide layer from the GaP surface was not stripped off completely in the chosen etching interval, which influences the current conduction mechanisms.

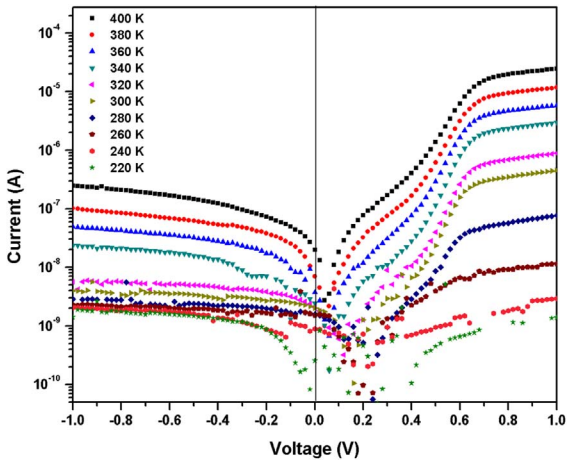

Fig. 8. The forward and reverse I-V characteristics of gamma irradiated Au/n-GaP Schottky diode in the temperature range 220–400 K.

The modified TE equation incorporating the native oxide interfacial layer is given as [36,38,39]:

$$I = I_0\left[\exp\left(\frac{q(V - IR_S)}{\eta kT}\right)\right]\left[1 - \exp\left(\frac{-q(V - IR_S)}{\eta kT}\right)\right] \quad (1)$$

where η is the ideality factor and I_0 is the reverse saturation current given as:

$$I_0 = AA^*T^2\theta_n \exp\left(-\frac{q\phi_{b0}}{kT}\right) \quad (2)$$

where,

$$\theta_n = \exp(4\pi/h)(2m^*)^{1/2} = \exp(-a\chi^{1/2}\,\delta) \quad (3)$$

Here, χ is the mean barrier height presented by the thin interfacial film and δ is the thickness of the interfacial insulator layer. The forward *I–V* characteristics of the gamma irradiated Au/n-GaP Schottky diode in the temperature range of 220–400 K and their best fit according to Eq. (1) are shown in Fig. 9.

The fitting parameters were zero bias barrier height (ϕ_{b0}), ideality factor (η), series resistance (R_s), χ and δ. The value of δ is calculated to be 10.2 nm from the fitting procedure. The experimental data in the 400–280 K range fit well to Eq. (1) in the higher bias regions, but deviate largely in the lower bias region due to excess current. However, it was found that the TN mechanism satisfactorily explains the low bias behaviors according to the equation given by [40]:

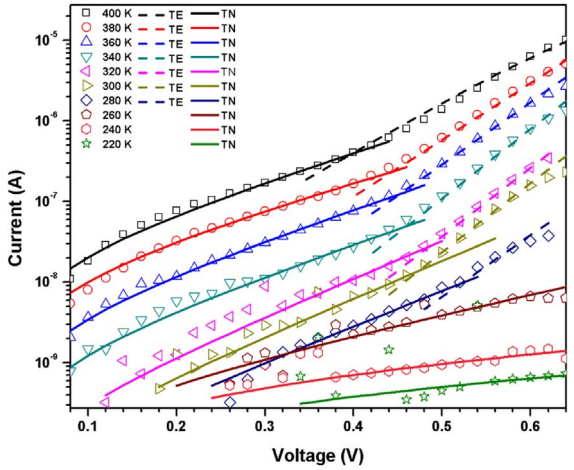

Fig. 9. The experimental and simulated I-V characteristics of γ-ray Irradiated Au/n-GaP Schottky diode at different temperatures. Here, the TE represents fit with Eq. (1) and TN represents fit with Eq. (4).

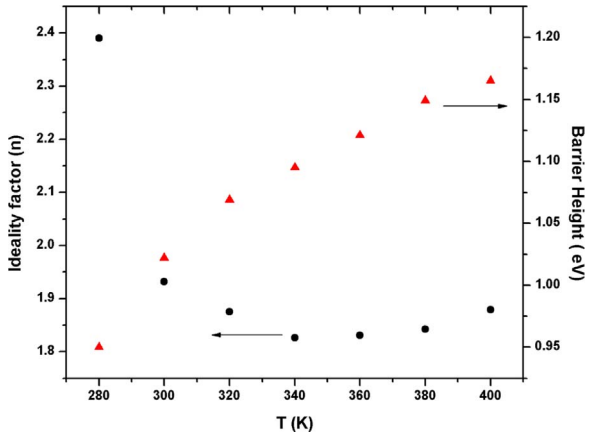

Fig. 10. Temperature dependence of ideality factor and zero-bias apparent barrier height for γ-ray irradiated Au/n-GaP Schottky diode.

$$I = I_{0TN}\left[\exp\left(\frac{q(V - IR_S)}{E_0} - 1\right)\right]\left[1 - \exp\left(\frac{-q(V - IR_s)}{kT}\right)\right] \quad (4)$$

where, I_{0TN} is the TN saturation current and E_0 is the TN parameter defined as [40]:

$$E_0 = E_{00}\coth(qE_{00}/kT) \quad (5)$$

Here E_{00} is the characteristic tunneling energy that is related to the tunneling transmission probability. The *I-V* curves are simulated using Eq. (4) with I_{0TN} and E_{00} as input parameters and are shown in Fig. 9. The figure reveals that in the 280–400 K temperature region the effective conduction process in the lower bias is TN, which gets gradually dominated by TE at higher bias. This is similar to the pristine sample in the range 400–260 K [36]. However, in contrast to the TE mechanism in pristine, as the temperature decreases TN mechanisms prevail in the whole chosen bias range. This shows the presence of newly formed defects by gamma irradiation that promotes tunneling [48]. Its presence unveils and becomes significant only when the freezing effect of TE carriers takes place at low temperatures.

In Fig. 10, it is observed that the value of ϕ_{b0} increases with the increase of temperature. At 300 K its value is 1.02 eV, whereas 0.95 eV was reported for the pristine sample [36].

The value of n initially decreases with the increase of temperature up to 340 K and remains more or less same up to 380 K. This is a usual feature for majority of Schottky diodes. With further rise of temperature, the n value shows slightly increasing trend due to the presence of defect states. The presence of defect states enhance the recombination and leakage current at higher temperature which accounts for increase in ideality factor with increase of temperature [49,50]. The value of n at RT is 1.93, which is much higher than 1.13 for the pristine sample. Similar higher values of n at other temperatures are also observed which strongly suggest the formation gamma induced additional defects promoting recombination and leakage current.

The fitted values of E_{00} and I_{0TN} at different temperatures are given in Fig. 11. The tunneling mechanisms are categorized into two types viz. the thermionic field emission (TFE) and the pure tunneling (TN) [39]. The E_{00} value is comparable to kT/q in the temperature range 280–400 K suggesting the occurrence of TFE mechanism in this range. However, below 280 K the TN mechanism dominates as the E_{00} is much larger than kT/q, which is also evident from the fit in Fig. 9. Additionally, the figure also shows increase in I_{0TN} with temperature. The minority carrier density generally increases with the rise of temperature, which results in the increase of I_{0TN}.

The values of R_s, extracted at each temperature from the fitting procedure obeying Eq. (1) is shown in Fig. 12. It increases with the decrease of temperature, which generally occurs due to carrier freezing effect at lower temperatures. The high value of R_s can be due to

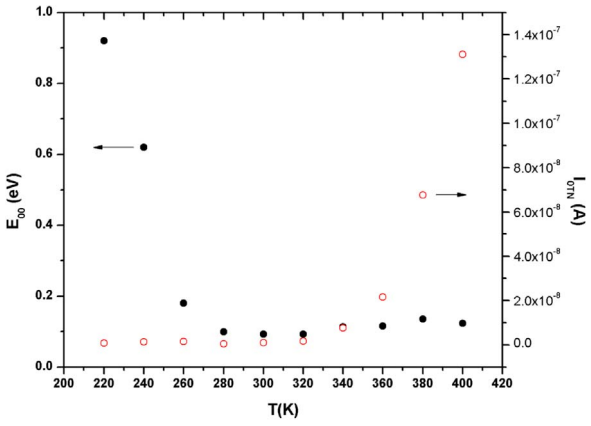

Fig. 11. Temperature dependence of E_{00} and I_{0TN} for γ-ray irradiated Au/n-GaP Schottky diode.

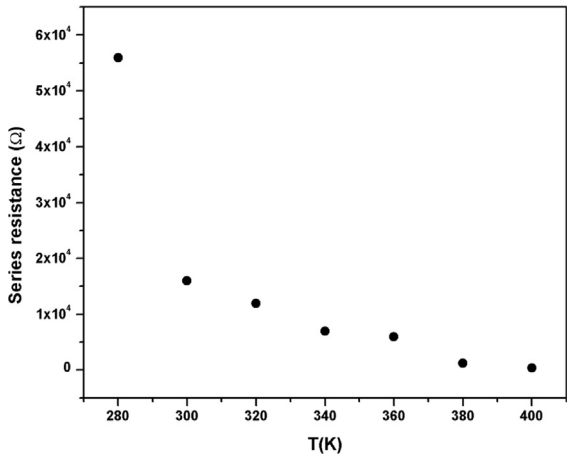

Fig. 12. Temperature dependence of series resistance for γ-ray irradiated Au/n-GaP Schottky diode.

reduction in charge carrier mobility across the interface, possibly due to radiation induced increment in interface state density, which acts as scattering centers.

4. Conclusions

The investigation of ^{60}Co gamma irradiation effect on the capacitance/conductance and transport properties of previously studied [36,37] Au/n-GaP Schottky diode was performed in the temperature range 220–400 K. The frequency dispersion in the high reverse bias region signifies a change in deep defect levels after gamma irradiation. The $G_p/\omega - f$ reveals the presence of additional interface state defects with independent time constant. The value of N_{ss} is of the order of 10^{13}/ eV cm^2 at 300 K, which is an order higher than the pristine sample. A reduction in the span of τ is also observed, which indicates the annihilation of some long lived interface states. The non-Debye type relaxation process has been observed from the $G_p/\omega - f$ plot. The shorter relaxation time with increasing temperature indicates an increase in the mobility of carriers among the trap states. Furthermore, defect annihilation processes were also observed at higher temperature as indicated by decrease in N_{ss} value with increasing temperature. The Arrhenius plot of σ_{ac} shows the presence of both shallow and deep trap states with activation energies 0.073 eV and 0.21 eV respectively. The evaluated transport mechanism reveals TE in the range 280–400 K in the high bias region. However, its deviation at low bias is found to be TN, suggesting the influence of interface state defects that promotes tunneling. The complete domination of TN below 280 K, in contrast to

pristine, confirms the formation of extra irradiation induced defects. The temperature variation of ϕ_{b0}, n, I_{0TN}, E_{00} and R_s also confirm the effect of irradiation induced defects in the transport properties. Even though some interface states with long relaxation time were annihilated, the overall defect state density, both interfacial and deep level, has been enhanced upon irradiation. Hence, it is concluded that the formation of these defects due to gamma irradiation plays a vital role in the terminal properties of the device.

Acknowledgements

Authors are grateful for the technical supports from Mr. S.R Abhilash and Mr. Birendra Singh (IUAC, New Delhi, India). NS thanks ISM, Dhanbad, India for the financial support under ISM-JRF scheme and AB thanks Department of Science and Technology, India for the financial support under Grant No: SB/FTP/PS-072/2013.

References

[1] R.C. Hughes, T.E. Zipperian, L.R. Dawson, R.M. Biefeld, R.J. Walko, M.A. Dvorack, J. Appl. Phys. 69 (1991) 6500.
[2] A.E. Belyaev, N.S. Boltovets, V.N. Ivanov, A.B. Kamalov, L.M. Kapitanchuk, R.V. Konakova, Ya Ya, Kudryk, O.S. Lytvyn, V.V. Milenin, Semicondutors 42 (2008) 453.
[3] Y. Nannichi, G.L. Pearson, Solid State Electron. 12 (1969) 341.
[4] Yu.V. Zhilyaev, E.A. Panyutin, L.M. Fedorov, Tech. Phys. Lett. 35 (2009) 808.
[5] A.N. Pikhtin, S.A. Tarasov, B. Kloth, IEEE Trans. Electron Devices 50 (2003) 215.
[6] Y.A. Goldberg, Semicond. Sci. Technol. 14 (1999) R41.
[7] M. Darnon, R. Varache, M. Descazeaux, T. Quinci, M. Martin, T. Baron, D. Muñoz, AIP Conf. Proc. 1679 (2016) 040003.
[8] X. Lu, S. Huang, M.B. Diaz, N. Kotulak, R. Hao, R. Opila, A. Barnett, IEEE J. Photovolt. 2 (2012) 214.
[9] P. Horley, Y.V. Vorobiev, V.P. Makhniy, V.M. Sklyarchuk, Phys. E: Low-Dimens. Syst. Nanostruct. 83 (2016) 227.
[10] C.C. Tin, Deep Level Transient Spectroscopy, John Wiley & Sons, 2012.
[11] D.C. Sheridan, G. Chung, S. Clark, J.D. Cressler, IEEE Trans. Nucl. Sci. 48 (2012) 2229.
[12] G.A. Umana-Membreno, J.M. Dell, G. Parish, B.D. Nener, L. Faraone, U.K. Mishra, IEEE Trans. Electron Dev. 50 (2003) 2326.
[13] H. Uslu, M. Yıldırım, S. Altındal, P. Durmus, Radiat. Phys. Chem. 81 (2012) 362.
[14] Ö. Güllü, M. Çankaya, M. Biber, A. Türüt, J. Phys. D: Appl. Phys. 41 (2008) 135103.
[15] N. Tuğluoğlu, S. Karadeniz, Ö.F. Yüksel, et al., Indian J. Phys. 89 (2015) 803.
[16] Y.S. Ocak, T. Kılıcoglu, G. Topal, M.H. Baskan, Nucl. Instrum. Methods A 612 (2010) 360.
[17] A. Bobby, N. Shiwakoti, S. Verma, P.S. Gupta, B.K. Antony, Mater. Sci. Semicond. Proc. 21 (2014) 116.
[18] A.P. Vyatkin, N.K. Maksimova, Soviet Phys. J. 26 (1983) 952.
[19] Y.J. Lin, Y.M. Chen, T.J. Cheng, Q. Ker, J. Appl. Phys. 95 (2004) 571.
[20] J. Racko, P. Benko, I. Hotovy, L. Harmatha, M. Mikolásek, R. Granzner, et al., Appl. Surf. Sci. 312 (2014) 68.
[21] O.Y. Olikh, IEEE Trans. Nucl. Sci. 60 (2013) 394.
[22] P. Krispin, J. Maege, Phys. Status. solidi 84 (1984) 573.
[23] P. Kamiński, R. Kozłowski, S. Strzelecka, A. Hruban, E. Jurkiewicz-Wegner, M. Piersa, Phys. Status Solidi C 8 (2011) 1361.
[24] T.A. Kennedy, N.D. Wilsey, J.J. Krebs, G.H. Stauss, Phys. Rev. Lett. 50 (1983) 1281.
[25] H. Xu, Phys. Rev. B 46 (1992) 12251.
[26] S. Das, S.K. Chaudhuri, K.C. Mandal, ECS J. Solid State Sci. Technol. 5 (2016) P3059.
[27] R.L. Dubey, S.K. Dubey, A.D. Yadav, D. Kanjilal, Int. J. Nanosci. 10 (2011) 105.
[28] R.L. Dubey, S.K. Dubey, A.D. Yadav, Indra Sulania, D. Kanjilal, Radiat. Eff. Defect. Solids 166 (2011) 743.
[29] V. Jadhav, M.D. Kirkire, S.K. Dubey, A.D. Yadav, A. Singh, F. Singh, D. Kanjilal, Radiat. Eff. Defect. Solids 168 (2013) 564.
[30] G.E. Zardas, Ch.I. Symeonides, P.C. Euthymiou, G.J. Papaioannou, P.H. Yannakopoulos, M. Vesely, Solid State Commun. 145 (2008) 332.
[31] E. Yu. Brailovskii, N.E. Grigoryan, G.N. Eritsyan, Phys. Status Solidi (a) 62 (1980) 648.
[32] V.S. Vavilov, R. Kh, Vagapov, M.V. Chukichev, Soviet Phys. J. 19 (1976) 722.
[33] E.M. Goldys, J. Barczynska, M. Godlewski, A. Sienkiewicz, B.J.H. Liesert, J. Appl. Phys. 74 (1993) 2287.
[34] P.S. Winokur, J.M. McGarrity, H.E. Boesch, IEEE Trans. Nucl. Sci. 23 (1976) 1580.
[35] T.P. Ma, Semicond. Sci. Technol. 4 (1989) 1061.
[36] N. Shiwakoti, A. Bobby, K. Asokan, B. Antony, Mater. Sci. Semicond. Proc. 61 (2017) 145.
[37] N. Shiwakoti, A. Bobby, K. Asokan, B. Antony, J. Vac. Sci. Technol. B 34 (2016) 051206.
[38] H.C. Card, E.H. Rhoderick, J. Phys. D. 4 (1971) 1589.
[39] S.M. Sze, Physics of Semiconductor Devices, 2nd ed., Wiley, New York, 1981.
[40] E.H. Rhoderick, R.H. Williams, Metal-semiconductor Contacts, 2nd ed., Clarendon Press, Oxford, 1988.
[41] S. Altındal, H. Uslu, J. Appl. Phys. 109 (2011) 074503.
[42] Q. Wang, J. Chen, H. Tang, X. Li, Semicond. Sci. Technol. 31 (2016) 065023.
[43] E.H. Nicollian, J.R. Brews, MOS (Metal Oxide Semiconductor) Physics and Technology, John Wiley & Sons, New York, 1982.
[44] P. Chattopadhyay, B. Raychaudhuri, Solid-State Electron. 36 (1993) 605.
[45] A. Sellai, P. Kruszewski, A. Mesli, A.R. Peaker, M. Missous, J. Nanophoton. 6 (2012) 0635021.
[46] O. Latry, A. Divay, D. Fadil, P. Dherbécourt, J. Semicond. 38 (2017) 0140071.
[47] K.Ç. Demir, S.V. Kurudirek, S. OZ, M. Biber, Ş. Aydogan, Y. Şahin, C. Coskun, Sur. Rev. Lett. 25 (2018) 1850064.
[48] M. Garg, A. Kumar, S. Nagarajan, M. Sopanen, R. Singh, AIP Adv. 6 (2016) 015206.
[49] S. Huang, B. Shen, M.J. Wang, F.J. Xu, Y. Wang, H.Y. Yang, et al., Appl. Phys. Lett. 91 (2007) 072109.
[50] A. Turut, K. Ejderha, N. Yildirim, B. Abay, J. Semicond. 37 (4) (2016) 0440011.